receiver noise temperature, but with necessary penalties of increased weight and complexity and limited portability. Current research is aimed at developing components that would enable all solid-state low-noise receivers to be constructed for operation at frequencies up to 350 GHz.

## Acknowledgment

The author wishes to thank N. Horner, who assembled the mixers and multipliers, G. Taylor, who fabricated the diplexer, Dr. S. Weinreb and R. Harris, for supplying the GaAsFET amplifiers, and Dr. R. Mattauch for providing the Schottky barrier diodes.

## References

[1] N. R. Erikson, "A 200–350 GHz heterodyne receiver," *IEEE Trans. Microwave Theory Tech.*, vol. MTT-29, pp. 557–562, June 1981.
[2] S. Lidholm and T. DeGraauw, "A heterodyne receiver for submillimeter wave astronomy," presented at 4th Int. Conf. Infrared and Millimeter Waves, (Miami, FL), Dec. 1979.
[3] P. F. Goldsmith and R. Plambeck, "A 230-GHz radiometer system employing a second harmonic mixer," *IEEE Trans. Microwave Theory Tech.*, vol. MTT-24, pp. 859–867, Nov. 1976.
[4] D. R. Carlson and M. V. Schneider, "Subharmonically pumped millimeter wave receivers," in *Conf. Dig., 4th Int. Conf. Infrared Millimeter Waves*, (Miami, FL,) Dec. 1979, pp. 82–83.
[5] J. W. Archer and R. J. Mattauch, "Low noise, single-ended mixer for 230 GHz," *Electron. Lett.*, vol. 17, pp. 180–181, Mar. 5, 1981.
[6] J. W. Archer, "Millimeter wavelength frequency multipliers," *IEEE Trans. Microwave Theory Tech.*, vol. MTT-29, pp. 552–557, June 1981.
[7] D. H. Martin and E. Puplett, "Polarized interferometric spectroscopy for the millimeter and sub-millimeter spectrum," *Infrared Phys.*, vol. 10, pp. 105–109, 1969.
[8] A. R. Kerr and R. J. Mattauch, and J. Grange, "A new mixer design for 140–220 GHz," *IEEE Trans. Microwave Theory Tech.*, vol. MTT-25, pp. 399–401, May 1977.
[9] H. Cong, A. R. Kerr, and R. J. Mattauch, "The low noise 115-GHz receiver on the columbia-giss 4-foot radio telescope," *IEEE Trans. Microwave Theory Tech.*, vol. MTT-27, pp. 245–248, Mar. 1979.
[10] D. L. Fenstermacher, "A computer-aided analysis routine including optimization for microwave circuits and their noise," NRAO Electronics Div. Internal Rep. 217, July 1981.
[11] J. Payne, NRAO, Tucson, AZ, private communication.
[12] S. Weinreb, D. L. Fenstermacher, and R. Harris, "Ultra low-noise, 1.2–1.7 GHz cooled GaAsFET amplifiers," *IEEE Trans. Microwave Theory Tech.*, vol. MTT-30, pp. 849–853, June 1982.
[13] J. Ondria, "Wideband mechanically tunable and dual in-line radial mode *W*-Band CW GaAs gunn diode oscillators," in *Proc. 7th Biennial Cornell Elec. Eng. Conf.*, Cornell Univ., (Ithaca, NY,) Aug. 14–16, 1979, pp. 309–32.

**John W. Archer** was born in Sydney, Australia, in 1950. He received the B.Sc., B.E. (Hons 1) and Ph.D. degrees from Sydney University in 1971, 1973, and 1978, respectively.

From 1974 and 1977 he was employed with CSIRO, Radiophysics Division, developing receiver and antenna systems for a radio interferometer operating at 100 GHz for high resolution solar radio astronomy. From 1977 to 1979 he was with NRAO's VLA program as a systems development and evaluation engineer. Since September 1979 he has worked in the NRAO Electronics Research and Development group in Charlottesville, VA. His current research interests are the development of low cost, efficient power sources at short millimeter lengths and the design of low-noise mixers to operate near 230 GHz.

# Short Papers

## A New Design for 1-CM Rutile Traveling Wave Masers

JAN ASKNE, MEMBER, IEEE, S. GALT, AND E. KOLLBERG

*Abstract* — **A new design of a rutile traveling wave maser is described. A dielectric rod waveguide is used as the interaction circuit. Essential mode coupling problems have been worked out in order to make the maser work properly. The advantage with this type of maser is the simplicity in the manufacturing and the very low insertion loss. A maser designed for the frequency range 26–29 GHz has been built, tested, and used in radio astronomical observations.**

Manuscript received February 11, 1982; revised March 29, 1982. This work was supported in part by the Swedish Board for Technical Development.

J. Anske and E. Kollberg are with the Research Laboratory of Electronics, Chalmers University of Technology, S-412 96, Cöteborg, Sweden.

S. Galt is with the Department of Physics, University of Toronto, Toronto, Ontario, Canada.

### I. Introduction

For *K*-band (18–26 GHz) and *Ka*-band (26–40 GHz) frequencies several maser designs have been described (e.g., [1], [2], [3]), and as far as low noise is concerned, no other device can yet compete with the maser in this frequency range. A flange noise temperature of about 15 K has been reported for a 500-MHz-wide *K*-band maser [1] and about 35 K for a 75-MHz-wide *Ka*-band maser [3]. The noise temperature in both cases is limited by the noise contribution of the input waveguide rather than the amplifier itself.

The present paper describes a maser design which can be

0018-9480/82/0800-1252$00.75 ©1982 IEEE

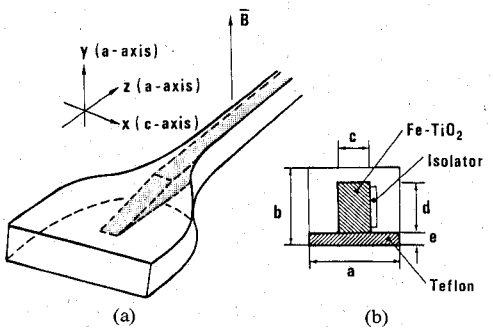


Fig. 1. Exploded view of the maser slow-wave structure demonstrating (a) the waveguide transition coupling section with the crystal and its orientation and (b) the cross-section parameters.

considered as a further development of the *Ka*-band image-line maser [3]. The new design described below has two advantages over the image-line maser: it has a much lower insertion loss (about 4 dB as compared to about 15 dB for the image-line maser over a length of 6 cm); and the manufacturing procedure is further simplified.

## II. General Considerations in the Maser Design

In Fig. 1 an exploded view of the maser slow-wave structure (SWS) is shown. The maser crystal (iron-doped rutile, $TiO_2$) has a magnetic field of 8 kG applied along the *a*-axis (Fig. 1). Two pump frequencies are fed to crystal through the output waveguide. The 1–2 transition is inverted when the 1–3 transition and 3–4 transitions at 60 and 40 GHz, respectively, are pumped to saturation. For more details see [3].

The signal wave grows exponentially while traveling from the input port to the output port of the SWS. In order to prevent feedback problems and oscillations, the portion of the amplified signal wave, which is reflected at the output port of the SWS, is absorbed by means of ferrimagnetic resonance absorption in the isolator applied to the side of the crystal (see [3] for more details).

The gain of a traveling-wave maser is described by the formula [4]

$$G = 27.3 \frac{S \cdot L}{\lambda_0} \cdot \left( \frac{1}{Q_m} - \frac{1}{Q_0} - \frac{1}{Q_{is}} \right) \text{dB}$$

where $S$ is the slowing factor of the slow-wave structure, $L$ the length of the SWS, $\lambda_0$ the vacuum wavelength of the signal, $Q_m$ the magnetic $Q$-value of the maser crystal, $Q_0$ the $Q$-value related to the insertion loss of the SWS, and finally $Q_{is}$ the $Q$-value related to the forward loss in the ferrimagnetic isolator.

The properties of the SWS determine the slowing factor (defined as the ratio of the velocity of light in vacuum ($c_0$) to the group velocity ($v_g = d\omega/dk$)) and the insertion loss ($\sim 1/Q_0$). The magnetic $Q$-value ($Q_m$) and the forward wave absorption in the isolator are determined by the properties of the materials used and the field configuration of the SWS. It was found that a strong RF-magnetic field along the *x*-axis (crystal *c*-axis) is advantageous for the maser crystal (Fig. 1), and simultaneously it is required to have as much RF magnetic field energy in the crystal (large filling factor) as possible. For optimum isolation, we require circularly polarized fields in the *xz*-plane at the surface of the rutile crystal where the isolator is situated. The sense of RF magnetic field polarization and the direction of the dc-magnetic field determine which direction of propagation is associated with large attenuation ($\sim$100 dB) and with a low attenuation ($\sim$2–3 dB). For the incoming signal wave, the isolator attenuation must of course be low.

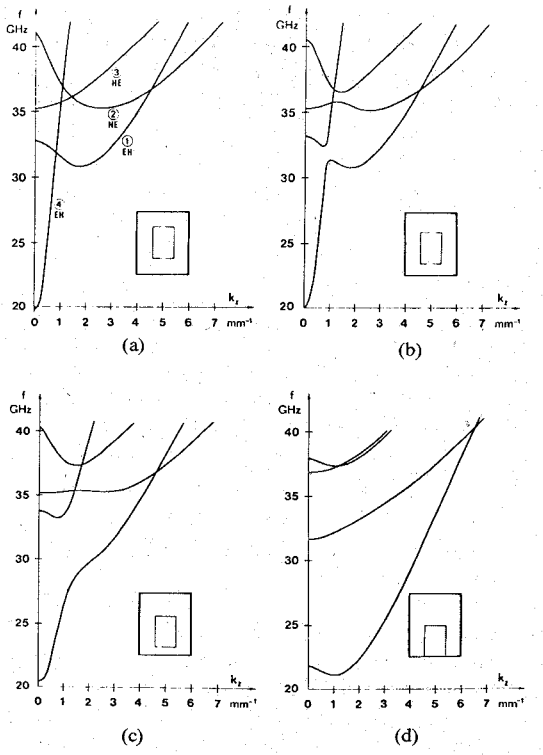


Fig. 2. Principle demonstration of the influence on the dispersion diagram due to the displacement of the crystal. $\epsilon_{rx} = 170$, $\epsilon_{ry} = 85$, $\epsilon_{rz} = 85$, $a = 1.30$, $b = 1.60$, $c = 0.55$, $d = 0.82$, and (a) $e = 0.39$, (b) $e = 0.29$, (c) $e = 0.19$, (d) $e = 0$. The calculations (cf. [8]) are based on an analysis of the coupling due to the crystal between $2 \times 5^2$ modes of the empty waveguide. The modes are designated in case (a) due to their symmetry properties [8].

The dimensions of the cross section of the structure affect: i) the slowing factor; ii) the filling factor and therefore $Q_m$; iii) the field configuration and therefore $Q_m$ and the isolation of the structure; and iv) the current in waveguide walls and therefore the insertion loss ($\sim 1/Q_0$) (the dielectric losses in the maser crystal can normally be neglected).

From this discussion it is obviously quite important to find a design procedure for optimizing a particular maser. In the following paragraphs we will discuss this problem in some detail.

## III. Description of the Slow-Wave Structure

The dispersion properties of all possible modes of propagation in the frequency range of interest were analyzed theoretically by two of the authors and their collaborators [5], [6], [8]. Since the theoretical analysis was in excellent agreement with the performed experiments, the theory formed an essential basis for understanding and designing the maser structure. Fig. 2 summarizes the theoretical results. Notice that mode ① is the mode utilized for amplification. Experimentally, we have tried the cases (a), (c), and (d) in various maser designs.

The image-line structure, case (d), has been used in maser applications by Kollberg and Lewin [3]. In this design, the surface of the rutile which is in contact with the metal waveguide is silvered (see [7]) and subsequently soldered to the metal waveguide. This procedure made it necessary to mill the waveguide structure out of titanium, since its coefficient of expansion matches that of rutile. Case (a) was tried next for the following reasons.

i) The insertion loss due to currents in the surface should decrease to a minimum, and in fact it is decreased from about 15 dB to about 4 dB.

ii) There is no need to silver the rutile and solder it to the waveguide, a procedure which needs considerable care.

iii) An ordinary brass material can be used since no matching of the thermal expansion coefficients is necessary.

iv) The brass can be goldplated much more easily than the titanium.

However, in case (a), the mode ④ is not used, but was found to cause considerable problems, since it will form a feedback circuit. Coupling between mode ① and mode ④, as well as between the input waveguide $TE_{10}$ mode and mode ④, should not be possible due to their respective symmetry properties. However, undesired asymmetries cannot be avoided due to tolerance problems, and the undesired coupling is a fact. Moreover, mode ④ barely interacts at all with the ferrimagnetic isolator, since its RF magnetic field is predominantly directed along the dc-magnetic field (see Fig. 1(b)). These circumstances mean that mode ④ constitutes a feedback circuit from the maser output port to its input port. In fact, it was found impossible to lower the coupling between mode ① and ④ enough, for oscillations not to occur even for a fairly low gain. Various schemes were tried to either quench or attenuate mode ④ but none was efficient enough to solve the problem.

Case (c) of Fig. 2 then seems to offer a way out of the problem observed for case (a). In breaking the symmetry of case (a) by lowering the crystal towards the bottom wall of the waveguide, a controlled coupling is deliberately introduced along the *whole* structure. Hence, modes ④ and ① are partly coupled together and as a result i) a frequency region is created where only one mode is propagated, and ii) the upper branch of the former mode ④ is now well attenuated by the isolator, since the field pattern is changed towards that of mode ②.

Experimentally, we have observed this effect by measuring the isolation, i.e., the attenuation of a signal traveling from the output towards the input. Hence, with the crystal placed in the center of the waveguide (case (a)), the coupling between modes ② and ④ resulted in an isolation of not more than 40 dB over a maximum of 2 GHz at a center frequency of 30 GHz. Since the gain obtained from the maser crystal, i.e., the electronic gain, is almost as large for the backward direction as for the forward direction (see [3]), this isolation is barely enough for an electronic gain of 15 dB. This means a net gain of about 5 dB, since the total insertion loss sums up to about 10 dB (see below).

However, when the configuration of Fig. 1(b) was tried, the isolation increased to more than we could measure (60 dB). In fact, since the electronic gain was of the order 40 dB, we can certainly conclude that the isolation was considerably more than 80 dB.

## IV. Results

The maser structure was made of brass and goldplated. The coupling section (compare Fig. 1(a)) is essentially a taper section from a reduced-height wave guide about 6.3 mm long. The height of the taper section is only a few hundredths of a millimeter higher than the top surface of the rutile (see below), which is essential for accomplishing a good coupling. The height is abruptly increased to that of the SWS (dimension $b$) after a few wavelengths in the SWS. The crystal is just linearly tapered, as indicated in Fig. 1(a). The exact form of the width-reducing taper is not very critical. In the structure itself, the crystal is supported by a sheet of teflon 0.05 mm thick ( = dimension $e$) and surrounded by very low dielectric constant plastic foam material, which holds the crystal in place.

The maser is designed for operation in the 26–29-GHz band,

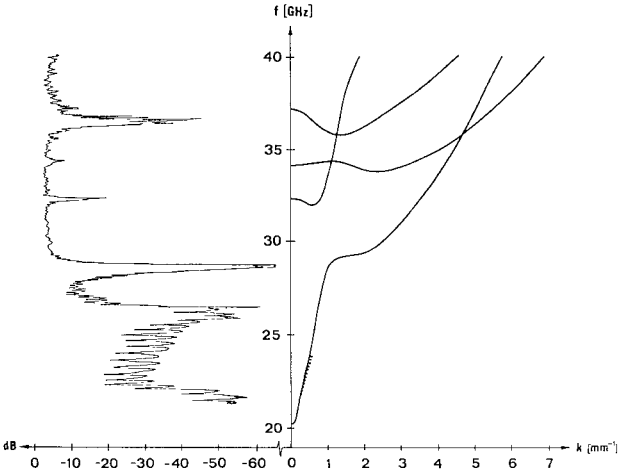


Fig 3. Experimental results demonstrating insertion loss (left-hand part) and corresponding experimental dispersion diagram ( · · · · · · ) of structure used for maser construction (right-hand part) at room temperature. Calculated dispersion diagram (neglecting teflon sheet) based on $2\times10^{2}$ modes is illustrated in right-hand part for $a=1.30$, $b=1.62$, $c=0.57$, $d=0.92$, and $e=0.14$.

and has the following cross-sectional dimensions: $a=1.30$ mm; $b=1.62$ mm; $c=0.57$ mm; $d=0.92$ mm.

Maser experiments were performed using the dewar and waveguide assembly designed for a 30–35-GHz maser system, which was found not to be optimum for the present maser. The transmission curve and dispersion of the structure alone at room temperature is shown in Fig. 3. The insertion loss of the maser structure (3 dB) is more than 10 dB less than that of an image-line maser for the same frequency region. For the complete maser, there is a further attenuation of about 10 dB mainly caused by the output waveguide (4 dB) and the diplexing system for the signal and pump frequency at the maser output (4 dB). The isolator forward attenuation adds another 2.5 dB yielding a total of 15-dB attenuation.

When cooled to liquid-helium temperatures, the relative dielectric constant of rutile increases with a factor of 1.46 while the useful frequency band moves from about 30–34 GHz (Fig. 3) to 26–29 GHz. Also the insertion loss decreases somewhat.

At 4.2 K, the electronic gain was about 22 dB yielding a net gain for the structure of about 19 dB, but a system gain of only 7 dB. At 2 K, the electronic gain was 39 dB yielding a structure gain of 36 dB and a system net gain of 22 dB. The 3-dB bandwidth of the 2 K amplifier was 80 MHz. The tunability is limited to the frequency range 26.5–29.0 GHz. The upper frequency limit is determined by oscillations caused by feedback problems (compare Fig. 3). The lower frequency was limited by the triplexer. We may expect that the lower frequency should otherwise be at 24.5 GHz.

The maser system has recently been tested successfully in the 20-m, millimeter-wave telescope at Onsala Space Observatory, and during this first test period several new spectral lines have been found. The noise temperature of the maser system (at the room-temperature input waveguide flange) is about 35 K.

## V. Discussion and Conclusion

The electronic gain per unit length of the maser is somewhat less than that of the 29–35-GHz image-line masers reported in [3]. The main reason is that there is a lower filling factor due to a thinner crystal and possibly also due to a modified field pattern caused by the mode mixing between modes ① and ④.

Obviously, the system performance should increase consider-

ably by decreasing the insertion loss of the output waveguide. This could be reduced by gold plating the inner surfaces or making the assembly from copper and by feeding the pump-power to the maser crystal in a more efficient way. However, it may also be possible to further improve the structure by i) increasing the length (now 5-cm active length). Compare the NRAO maser [1], which is 50 cm long; and/or ii) trying other cross sections, e.g., decreasing $e$ further to get more tuning range (but less slowing) as indicated in Fig. 2(c).

If increasing the length of the maser is considered, it is necessary to carefully align the rutile crystal axes to within about $\pm 3°$ in order not to deteriorate the electronic gain by more than about 5 percent.

Since the maser is cooled by immersion in liquid helium, there is no need to take special precaution to have a good thermal contact between the rutile crystal and the metal structure. In a closed-cycle refrigerator, the situation is different and the teflon sheet should be replaced by a material with a high thermal conductivity such as sapphire.

ACKNOWLEDGMENT

We would like to thank C. O. Lindström for much help in performing various measurements.

REFERENCES

[1] C. R Moore, "A $K$-band maser with 500-MHz bandwidth," *IEEE Trans. Microwave Theory Tech* vol. MTT-28, *pp.* 149–151, 1980.
[2] K. S. Yngvesson, A. C Cheung, M. F. Chui, A. G. Cardiasmenos, S. Y Wang, and C. H. Townes, "$K$-band traveling-wave maser using ruby," *IEEE Trans. Microwave Theory Tech.*, vol MTT-24, pp. 711–717, 1976
[3] E. L. Kollberg and P T. Lewin, "Traveling-wave masers for radio astronomy in the frequency range 20–40 GHz," *IEEE Trans. Microwave Theory Tech.*, vol. MTT-24, pp. 718–725, 1976.
[4] A. E. Siegman, *Microwave Solid-State Masers New York: McGraw-Hill*, 1964.
[5] T. Lewin, J. Järnmark, and E. Kollberg, "Theoretical and experimental evaluation of high perimittivity dielectric rod waveguides," *Int. J. Electron.*, vol. 49, pp. 147–159, 1980.
[6] J. Askne, E. Kollberg, and L. Pettersson, "Analysis of a waveguide partially filled with a dielectric material," in *Proc. 10th Euro. Microwave Conf.* (Warszawa), 1980.
[7] T. Lewin and E. Kollberg, "Rutile traveling wave masers for the frequency range 20–45 GHz," Res. Report 134, Research Laboratory of Electronics, Chalmers University of Technology, Göteburg, Sweden, 1978.
[8] J. Askne, E Kollberg, and L. Pettersson, "Propagation in a waveguide partially filled with an anisotropic dielectric material," *IEEE Trans. Microwave Theory Tech.*, vol. MTT-30, pp. 795–799, May 1982.

# Determination of Microwave Transistor Noise and Gain Parameters Through Noise-Figure Measurements Only

GIOVANNI MARTINES AND MARIO SANNINO

*Abstract*—**A novel method for measuring noise and gain parameters of linear two-ports solely from noise-figure measurements is applied here to perform noise and gain characterization of microwave transistors versus frequency and collector current in $S$-band.**

**The method results in a simpler procedure and improved accuracy compared to conventional methods. In addition, a technique to estimate the loss of the input tuner of the measuring setup is presented, which yields a further improvement in accuracy.**

**As experimental verification, the noise and gain parameters of a microwave transistor versus collector current in the 2–4-GHz frequency range are reported.**

Manuscript received February 11, 1982; revised April 7, 1982. This work was supported in part by the Italian National Research Council

The authors are with the Instituto di Eletrotecnica ed Elettronics, Viale delle Scienze, 90128 Palermo, Italy.

## I. INTRODUCTION

At microwave frequencies it is convenient to write the two-port noise figure $F$ in terms of input termination (or source) reflection coefficient $\Gamma_s = \rho_s \exp j\vartheta_s$ in the form [1], [2]

$$F(\Gamma_s) = F_0 + 4N_n \frac{|\Gamma_s - \Gamma_{0n}|^2}{(1-|\Gamma_s|^2)(1-|\Gamma_{0n}|^2)} \tag{1}$$

where $F_0$ (the minimum noise figure), $\Gamma_{0n} = \rho_{0n} \exp j\vartheta_{0n}$ (the optimum source reflection coefficient), and $N_n$ (a terminal invariant parameter), are the four microwave noise parameters.

Similarly, we can introduce the following relationship for the available power gain:

$$\frac{1}{G_a(\Gamma_s)} = \frac{1}{G_{a0}} + 4N_g \frac{|\Gamma_s - \Gamma_{0g}|^2}{(1-|\Gamma_s|^2)(1-|\Gamma_{0g}|^2)} \tag{2}$$

where $G_{a0}$, $\Gamma_{0g} = \rho_{0g} \exp j\vartheta_{0g}$, and $N_g$ are the four microwave gain parameters.

Based on standard methods of determining noise parameters established by the IRE [3], modernized computer-aided techniques have been developed [4], [5] and their drawbacks and improvements have been discussed [2], [6], [7].

The characterization of microwave transistors versus frequency and bias conditions in the $S$-band reported in this paper are obtained through a measuring technique which overcomes the usual time-consuming inconveniences.

Usually the device noise figure $F(\Gamma_s)$ is computed by means of the well-known Friis formula

$$F_m(\Gamma_s) = F(\Gamma_s) + \frac{F'-1}{G_a(\Gamma_s)} \tag{3}$$

where $F'$ and $F_m(\Gamma_s)$ represent the noise figure of all stages subsequent to the device and the overall measured noise figure, respectively.

From (3) it is obvious that the accuracy with which $G_a(\Gamma_s)$ is measured influences also the determination of $F(\Gamma_s)$ and consequently, of the device noise and gain parameters.

In the method proposed, both noise- and gain-parameter sets are simultaneously determined solely through noise-figure measurements. This simplifies the measurement procedure considerably and avoids separate instruments for the gain measurement. Further, since the device under test is driven at the noise level, nonlinearity effects are avoided; this improves the measurement accuracy by comparison with the methods which use signal generators to measure the gain. Commercial instruments for the simultaneous measurement of noise figure and gain of a device driven by a noise source are available at present (e.g., Hewlett-Packard mod. 8970 and Ailtech mod. 7380). These instruments, however, have been designed for measurements on the well-matched devices and, consequently, they are not convenient for transistor characterization. Furthermore, the method presented is believed to be more accurate in that the noise figure and gain of the device are determined through a fitting procedure of redundant experimental data.

It is noteworthy that for a correct measurement of $F_m(\Gamma_s)$, the

0018-9480/82/0800-1255$00.75 ©1982 IEEE